IEEE Access
Multidisciplinary | Rapid Review | Open Access Journal

Received 14 September 2022, accepted 4 October 2022, date of publication 6 October 2022, date of current version 13 October 2022.

Digital Object Identifier 10.1109/ACCESS.2022.3212746

RESEARCH ARTICLE

Comparative Analysis of Partial Discharge Detection Features Using a UHF Antenna and Conventional HFCT Sensor

JEAN PIERRE UWIRINGIYIMANA[1], UMAR KHAYAM[1], (Member, IEEE), SUWARNO[1], (Senior Member, IEEE), AND GIAN CARLO MONTANARI[2], (Life Fellow, IEEE)

[1]School of Electrical Engineering and Informatics, Institut Teknologi Bandung, Bandung 40132, Indonesia
[2]Center for Advanced Power Systems, Florida State University, Tallahassee, FL 32306, USA

Corresponding author: Jean Pierre Uwiringiyimana (upeter1@yahoo.fr)

This work was supported by the World Class Research Program, Kemdikbudristek, Indonesia.

ABSTRACT This article presents a design of ultra-high frequency (UHF), ultra-wide band (UWB) antenna used for partial discharge (PD) detection on high voltage and medium voltage power system equipment. The proposed UHF antenna has a working frequency band of 1.2GHz-4.5GHz, covering a total bandwidth of 3.3GHz with a return loss of less than -10dB in the entire antenna's operating frequency. The computer simulation technology (CST) Microwave Studio software was used to design, simulate and optimize the proposed antenna. Upon simulation and optimization process, the antenna prototype was fabricated on the FR-4 substrate of 1.6 mm thickness and dielectric permittivity of 4.4. This antenna has a compact size of 100mm $\times$ 100mm.The radiating patch and the ground plane of this antenna are made of annealed copper whose thickness is 0.035mm. The simulations and measurement results for the proposed antenna are in a good agreement, and the return loss of this antenna is less than -10dB with voltage standing wave ratio, VSWR, < 2 within the frequency range of interest. The proposed antenna performance in PD sensing is compared with a commercial high-frequency current transformer, HFCT. To validate the sensitivity performance of the designed antenna, experimental PD measurements were carried out by using an epoxy slab inserted between two parallel plates electrode model, in order to generate surface discharge on the insulator, and using a needle-plate electrode configuration to generate corona discharge in transformer oil. Based on PD measurement results, it was shown that the designed antenna has a high sensitivity, which make it a suitable candidate for UHF partial discharge monitoring on high voltage and medium voltage power assets.

INDEX TERMS Surface discharge, corona discharge, UHF antenna, HFCT, UHF PD monitoring.

I. INTRODUCTION

Insulation health of high voltage power equipment is a fundamental indicator that determines power system reliability. Any significant aging process or defect in the insulation system of HV or MV equipment may strongly affect electrical asset safe operation and reliability. Insulation defects may cause high electric field within the insulation system of a power equipment, which will in turn cause partial discharge (PD) activity in that portion of the insulation. The occurrence of PD activity on high voltage (HV) and medium voltage (MV) assets causes accelerated degradation of the insulation, which will generally result in insulation failure and possibly premature and unplanned breakdown of the HV and MV power equipment [1]. Indeed, PD phenomenon has been categorized as the main threat of the electrical insulation and at the same time the primary indicator of the insulation weakness [2], [3], [4].

Different types of insulation defects are associated with different types of partial discharges. For instance, gas-filled cavities within the solid insulation cause internal discharge, protrusion near a high voltage conductor generates corona

The associate editor coordinating the review of this manuscript and approving it for publication was Pavlos I. Lazaridis.

discharge and contaminated insulator surface or defective outer semiconductor layer initiate surface discharge [5]. The health assessment of electrical insulation requires a rapid diagnostic method capable of detecting, localizing and identifying these insulation defects at an early stage to prevent any premature breakdown of the HV or MV power equipment.

To assess the insulation condition of the power system equipment, the partial discharge (PD) level should be monitored continuously to prevent any unplanned breakdowns in advance, thus helping to schedule maintenance and repair plans before any unwanted power outages and equipment breakdown may take place [6]. PD activity is usually accompanied by some physical, acoustic and chemical phenomena in various energy forms, namely, electromagnetic (EM) wave radiations, impulse current, acoustic emission (pressure waves), chemical reactions, heat and light that are detected by specific sensors, such as VHF/UHF sensor, acoustic sensor (piezoelectric sensor), HFCT sensor, dissolved gas sensor, UV and infrared cameras [7], [8]. The UHF method, commonly known as electromagnetic method, can be used for online PD monitoring of, e.g., rotating machines or switchgears, based on its capability to capture undisturbed (in terms of bandwidth) PD signals compared to the ultrasonic method and to the conventional method or electrical method (IEC 60270 standard method) [9], [10]. In addition, UHF method has proven to have a high signal-to-noise ratio (SNR) since its detection frequency ranges from 300 MHz to 3GHz, which enables this method to reject some ambient noises (e.g. corona noise whose frequency is below 300MHz). Unlike some electrical methods that requires a direct contact to the HV or MV equipment under test (as capacitive couplers or transient earth voltage, TEV, sensors), the UHF method does not require any physical contact with the object under test. In addition, UHF method requires few sensors (typically 3 sensors) for PD source localization [11].

The UHF method is supported by sensors such as UHF probes and UHF antennas to detect PD activity. External and built-in UHF sensors are used to detect PD signals radiated by PD source in gas-insulated substation and switchgears, GIS, as well as power transformers. However, built-in (internal) sensors have the advantages over external sensors in terms of higher sensitivity, signal-to-noise ratio (SNR) and immunity against external electromagnetic interferences [12], [13], [14], [15]. As an example, for PD detection on power transformers, UHF sensors (antennas) can be inserted into the power transformer via the oil drain valves or placed at dielectric windows. For insulation reliability purpose, the detection distance between an internal sensor and the main insulation (which is inversely proportional to measurement sensitivity) should be long enough to avoid the risk of introducing additional premature failure risk. That is why most of the UHF antennas that are designed to be used as internal sensors inside HV or MV equipment have mostly planar shape (UHF planar antennas) in order to minimize their height [16].

Since an UHF antenna play a fundamental role in the UHF PD monitoring system for insulation defect detection, localization and identification, it should be designed to have high sensitivity (high gain and directivity), high signal-to-noise ratio (SNR) and wide bandwidth which enables high detection accuracy with minimum signal distortion.

Many studies on UHF PD antenna design have been conducted to detect PD activity on HV or MV power equipment. For example, Qi et al. [16], designed an ultra-wide band metal-mountable antenna for UHF partial discharge detection. This antenna has a bandwidth of 400MHz-3GHz. In [7], a circularly-polarized UHF PD antenna working in the frequency range from 0.6 GHz to 1.7 GHz has been proposed, but its sensitivity for PD detection was not analyzed. In publication [8], a radio frequency(RF) antenna whose frequency band is 1GHz-2GHz was proposed for PD measurement on defective ceramic insulators in laboratory and on outdoor HV transmission lines. This antenna was able to detect PD at a distance of 2.5m from the 45kV energized insulators. A two-arm equiangular spiral antenna having a frequency band of 0.5GHz to 3.5GHz was designed and optimized as a PD sensor for GIS in [17], but only simulation results were presented. In [18] a comparative study on three different Hilbert fractal antennas implemented for PD detection on oil-filled tank is presented. Performance was analyzed based on the SNR of the UHF signals captured by each antenna. Wang et al [19], have recently proposed an Archimedes spiral antenna for partial discharge detection of inverter-fed motor insulation. This UHF antenna (whose frequency range is from 0.5GHz to 2GHz) has shown its potential in detecting PD under repetitive impulsive voltages with short rise times and high frequency voltage.

However, some of these antennas still have narrow bandwidth and low gain, that affect their sensitivity performance. The work presented here brings an innovative contribution through a design of UHF antenna having an ultra-wide band (UWB) with a high gain in the frequency range of interest for PD occurrence. The high gain, high directivity and wider bandwidth of this antenna enable it to reach higher sensitivity to PD pulse signals irradiated by insulation defects under high electric field. The bandwidth and the gain improvement of the antenna was achieved by cutting the circular patch from its top toward its center. Another technique used to improve the antenna bandwidth is creating a U-shaped slot in the ground plane of the antenna. The technique of introducing a slot into the ground plane of the antenna is also known as defected ground structure method, and it has been widely used in antenna design engineering for several applications [20], [21], [22], [23]. The proposed UHF antenna has, therefore, an ultra-wide band frequency response ranging from 1.2GHz to 4.5GHz, covering an impedance bandwidth of 3.3GHz with a voltage standing wave ratio (VSWR) less than 2 and a return loss below -10dB within the frequency range of interest.

Simulation and optimization process of this UHF antenna was presented in our previous research [24], where preliminary work was conducted by implementing the designed antenna for PD detection using the needle-plate electrode

model to generate corona discharge in air. To further evaluate the sensitivity performance of the designed UHF antenna in detecting PD activity in different insulation media and different types of insulation defects (PD sources), this article focuses on performing the comparative analysis of partial discharge detection and measurement on both air-insulated and oil-insulated power equipment. To support the validity and sensitivity performance of the proposed antenna design, a commercial high frequency current transformer (HFCT), were used simultaneously with this UHF antenna in detecting PD through the laboratory experiments.

The sections of this article are organized as follows: Section II describes antenna design; Section III is about antenna fabrication and measurement results using the vector network analyzer. Section IV shows the laboratory experiments for the antenna sensitivity validation in detecting the PD-induced electromagnetic waves radiated by the insulation defect (PD source) in air insulation and transformer oil insulation. Lastly, Section V gives the conclusions emphasizing the validity and contribution of this study.

II. ANTENNA DESIGN AND SIMULATION

A. INITIAL ANTENNA DESIGN

The initial design of proposed antenna is a circular microstrip antenna working in the UHF range (300MHz-3GHz) which is the frequency range of interest for PD signals spectrum frequency. The advantage for choosing this kind of circular antenna design is that it can easily be optimized to cover a wider bandwidth with a compact size. In addition, the circular patch antennas have an omnidirectional radiation patterns enabling the antenna to detect PD signals originating from all directions. For instance, when the circular microstrip antenna are used to detect PD in a substation or inside a power apparatus such as transformers, the omnidirectional antennas are preferable since the PD source location is generally not known [25]. The initial circular microstrip antenna was modeled on an FR-4 substrate having a relative permittivity of 4.4 (with dielectric loss tan $\delta = 0.02$) and a thickness of 1.6mm. The initial antenna design has an operating frequency range of 1.2GHz-2.4GHz, having 1200MHz bandwidth coverage, below -10dB.

Figure 1 depicts the geometry of the initial antenna design, while its parameters are tabulated in table 1. The antenna is composed by a radiating circular patch at the top of the substrate and a partial ground plane at the bottom of the substrate. The microstrip feedline was used to link the circular patch to the ground plane.

As shown in table 1, the dimensions of the initial antenna design are 100mm $\times$ 90mm $\times$ 1.6mm. For antenna simulation, copper with thickness 0.035mm was used as the conducting material for both radiating patch and ground plane.

Fig.2 displays the simulated S11 parameter for the initial antenna design. It is clearly seen that the frequency band of this antenna is from 1.2GHzc to 2.4GHz, covering an impedance bandwidth of 1200MHz, below -10dB with a return loss value of -34.5dB at a resonance frequency of 1.45GHz.

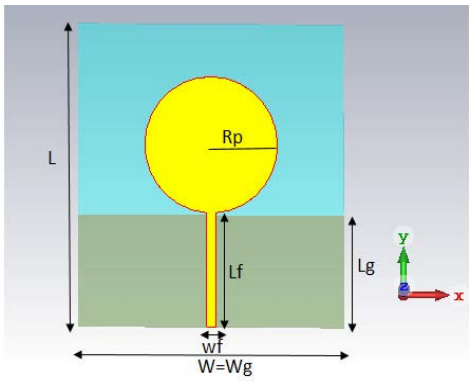

FIGURE 1. Geometrical structure of the initial design of circular microstrip antenna.

TABLE 1. Specification parameters for the initial antenna design.

Parameters		Values
Substrate length	L_p	100mm
Substrate width	W	90mm
Patch radius	Rp	22.5mm
Ground –plane length	Lg	37mm
Ground –plane width	Wg	80mm
Feedline length	Lf	40mm
Feedline width	Wf	1.53mm
Substrate relative permittivity	εr	4.4
Substrate thickness	h	1.6mm

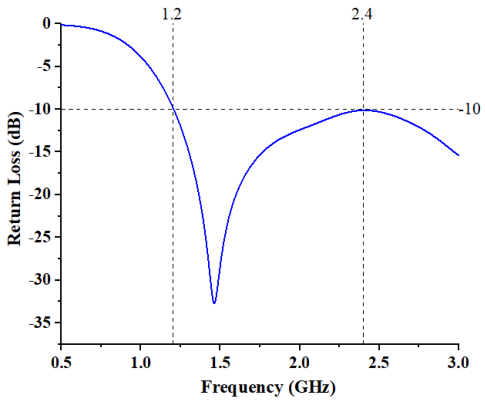

FIGURE 2. Simulated S11 parameter (Return loss) versus frequency for the initial antenna design.

Fig.3 reports the simulated gain and directivity versus frequency for the initial antenna design. Gain and directivity are among the most important parameters that have to be taken into consideration while designing an antenna: the higher gain and directivity, the higher radiation efficiency of the antenna. The radiation efficiency of the antenna is the ratio of the gain to the directivity. Best radiation efficiency values approach 1 (or 100%). From Fig. 3 (a), gain of the initial antenna design ranges from 1.8dB to 3.5dB, while directivity ranges from 2.4dB to 4dB in the antenna operating frequency. The simulated radiation efficiency of the initial antenna design is plotted in Fig.3 (b). It can be seen that

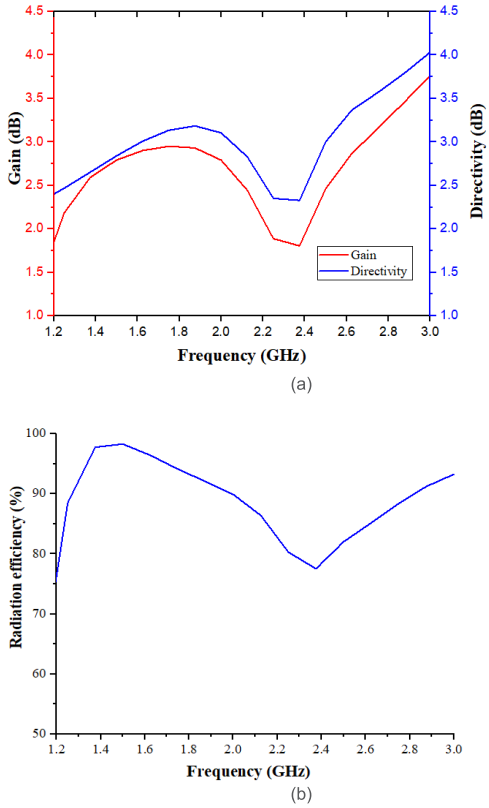

FIGURE 3. Simulated (a) gain and directivity (b) radiation efficiency versus frequency for the initial antenna design.

gain, directivity and radiation efficiency of the initial antenna design show fluctuating trend in the frequency range of interest. Therefore, the optimization of this antenna was required and implemented to increase gain and radiation efficiency, as well as to widen the bandwidth of the antenna, going towards the targeted frequency range of PD-pulse spectra (300MHz-3GHz).

B. OPTIMAL ANTENNA DESIGN

To broaden the antenna bandwidth as well as increasing its gain, directivity and radiation efficiency, a parametric optimization of the antenna was conducted. The structure of the initial antenna was modified by cutting the circular patch, which was truncated on its top [26]. Moreover, a U-shaped slot was etched into the ground plane behind the feedline, which contributes in improving the antenna bandwidth, gain and directivity [21], [20], [27].

Other parameters that were optimized are the length and the width of the feedline, ground plane length and width, as well as slot length and width. These parameters were varied to obtain the optimal antenna design operating in a frequency range of 1.14GHz to 4.5GHz, covering a total impedance bandwidth of 3.36GHz, below -10dB with a VSWR < 2 in the entire operating frequency band. Fig.4 shows the geometrical view of the optimal design of the proposed UHF antenna, while table 2 reports the parameter values for the optimal antenna design. The results for the simulated S11 parameter

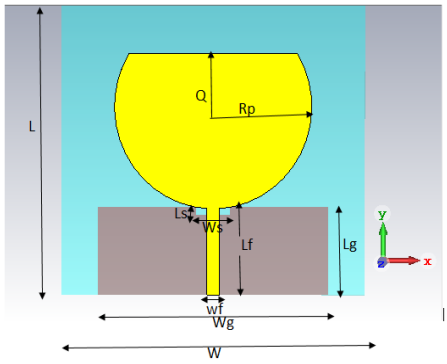

FIGURE 4. Geometrical structure for the optimal design of the proposed UHF antenna.

TABLE 2. Optimization parameters for the proposed UHF antenna [24].

Parameters		Values
Substrate length	L_p	100mm
Substrate width	W	100mm
Patch radius	Rp	32.5mm
Patch cut distance	Q	27mm
Ground –plane length	Lg	28mm
Ground –plane width	Wg	78mm
Feedline length	Lf	40mm
Feedline width	Wf	4mm
Slot length	Ls	2.5mm
Slot width	Ws	11mm
Substrate permittivity	εr	4.4
Substrate thickness	h	1.6mm

and the simulated VSWR of the optimized antenna are depicted in Fig.7 and Fig.8. In addition, for further analysis of the antenna sensitivity performance in detecting PD signals, the gain, directivity and radiation efficiency of the optimized antenna were simulated, as seen in Fig.5 (a) and (b). Contrarily to the results for the initial antenna design, it is clearly seen that the optimized antenna has higher gain and higher directivity.

Gain and directivity of the optimized antenna in the frequency interval of interest (1.14GHz-4.5GHz) are 1.4dB to 4.75dB (for gain), and 2.2dB to 4.7dB (for directivity), respectively, while those of the initial antenna were in the ranges of 1.8dB to 3.5dB (for gain) and 2.4dB to 4dB (for directivity), respectively.

It is evident that gain and directivity of the new antenna have been significantly improved, as seen in Fig.5 (a) with respect to the gain and directivity of the initial antenna (Fig.3 (a)). In addition, both gain and directivity of the optimized antenna have rising trend in the frequency range of interest, which indicates improved performance of the antenna to capture the PD signals with high radiation efficiency within the entire operating frequency band. The radiation efficiency of the optimal antenna design was also simulated, confirming a significant increase in radiation efficient, as seen in Fig.5 (b). For example, in the frequency range of 1.2GHz-3GHz, the radiation efficiency of the optimal antenna designed is almost constant and its value is

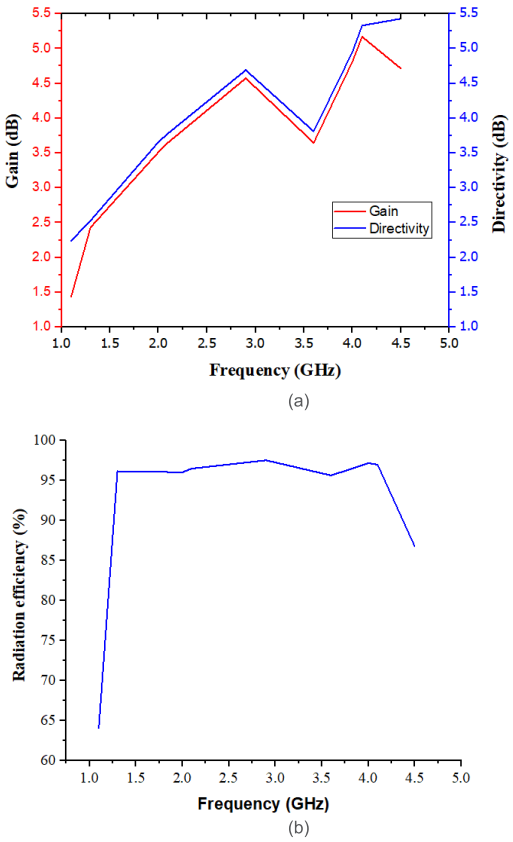

FIGURE 5. Simulated (a) gain and directivity (b) radiation efficiency versus frequency for the optimized antenna design.

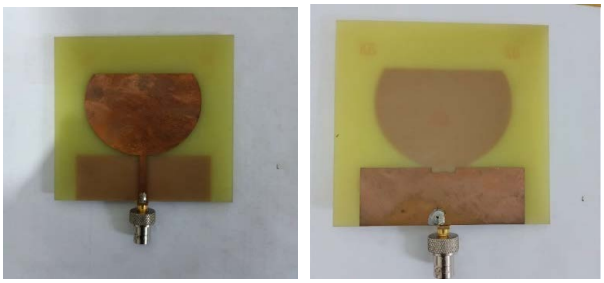

FIGURE 6. Fabrication of the optimized antenna prototype: (a) Front view (b) back view.

roughly 96%. This highlights that the optimized antenna has higher sensitivity in the frequency range of interest, compared to that of the initial antenna design (Fig.3 (b)). More details about simulation and optimization of the proposed antenna can be found in our previous research [24].

III. FABRICATION AND MEASUREMENT OF THE ANTENNA PROTOTYPE

Upon the simulation and optimization for the proposed UHF antenna, the prototype of the optimized antenna was fabricated and printed on the FR-4 substrate with relative permittivity of 4.4 (with a dielectric loss (tan δ) = 0.02). An electric conductor (annealed copper) with a thickness of 0.035mm was used for both radiating patch and ground plane. Fig.6 illustrates the fabricated optimized antenna. The SMA female connector and TNC male connector were used as a feed port (excitation point) between the antenna and the transmission line (50-Ohm coaxial cable that connect the antenna to the oscilloscope).

After the fabrication of the optimized antenna, a vector network analyzer (VNA), Cobalt Series C1220, was used to measure the antenna performance parameters, namely the reflection coefficient (return loss), voltage standing wave ratio (VSWR) and the impedance bandwidth. Fig.7 depicts the simulated and measured reflection coefficient (S11 parameter) and Fig.8.shows the simulated and measured VSWR of the proposed UHF antenna. Based on the simulation results, the designed antenna covers a working frequency range of 1.2GHz-4.5GHz, below −10dB (return loss less than −10dB) with a VSWR less than 2, while measured data indicate that the optimized antenna operates in the frequency range from 0.9GHz to 4.4GHz (covering a total bandwidth of 3.3GHz), below −10dB (return loss less than −10dB) with a VSWR less than 2.

The measurement results indicate that the VSWR is higher than 2 at the lower frequency range (frequency less than 0.9GHz), indicating the antenna's impedance mismatching at the lower frequency. However, a good impedance matching is

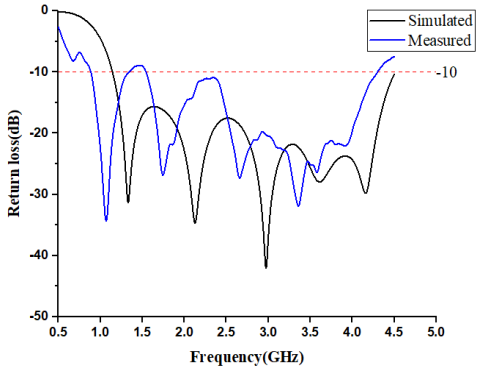

FIGURE 7. Simulated and measured reflection coefficient versus frequency for the designed UHF antenna.

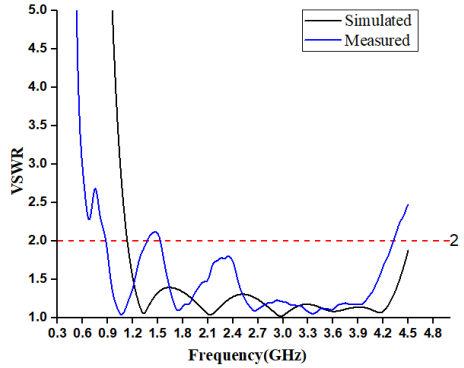

FIGURE 8. Simulated and measured VSWR versus frequency for the designed UHF antenna.

TABLE 3. Various types of antennas designed for PD detection from the literature.

Reference	Antenna name	Antenna Size	Antenna dielectric Substrate	Bandwidth below -10dB	Realized Gain range	Application for PD detection
This work	Circular microstrip patch antenna	100mmx100mm	FR-4	0.9GHz-4.4GHz	1.4dB-4.75dB	PD detection in both air insulation and transformer oil insulation
[16]	Elliptical Patch Antenna	282mmx242mm	FR-4	0.4GHz-3GHz	-6dB-11dB	Surface discharge PD detection on the contaminated insulator
[8]	Pyramid type Horn Antenna	Not given	Not given	1GHz-2GHz	14.5dB-18 dB	PD detection on ceramic insulators
[7]	Archimedean Spiral antenna	Diameter: 200mm	FR-4	0.6GHz-1.7GHz	0.3dB-4.6dB	PD detection experiment was not conducted, only simulation results are presented
[28]	Hilbert Antenna	70mmx70mm	FR-4	0.3GHz-1GHz	-12.8dB to -1dB	PD detection in transformer Oil Insulation
[29]	Loop-shaped antenna	138mmx89.5mm	FR-4	0.74GHz-1.5GHz	Not given	PD detection experiment was not conducted, only simulation results are presented
[30]	Archimedes spiral antenna	Diameter:190.3mm	Not given	0.9GHz-2GHz	2.5dB-7dB	PD detection generated by a pair of twisted wires energized using high voltage repetitive square wave generator
[31]	Octagonal patch antenna	124mmx77mm	FR-4	0.575GHz-4.5GHz	1.9dB-3.78dB	PD detection on 220kV GIS model

realized in the frequency range from 0.9GHz-4.5GHz where the VSWR is less than 2.

On the whole, comparing the characteristics of Figs. 7 and 8, it can be seen that simulation and measurement results are in a good agreement, except a slight shift in frequency towards lower frequency. The difference between simulation and measurement results for the optimized UHF antenna could be likely caused by fabrication errors, or even by the soldering material used to connect the SMA connector to the antenna. Indeed, the soldering material (usually lead) has different characteristics from the copper used as radiating patch and ground plane of the antenna. This may affect the frequency response of the antenna by displacing lower cut-off frequencies between the simulated and measured results (the soldering material was not considered in the simulations). The measurement errors inherent the vector network analyzer (VNA) might also cause discrepancies between simulated and measured results. In literature, it is claimed that both fabrication and measurement errors are the main cause of difference between the simulated and measured results [7], [16].

Various types of the antennas from the literature have been applied for PD detection in high voltage power apparatuses, as listed in table 3. As can be seen, most of the antennas have low gain, which can affect antenna sensitivity in detecting electromagnetic waves emitted by PD activity. In addition, some antennas were likely not implemented for PD detection through experiments to verify their sensitivity, because only simulation results were given in their studies [7], [29]. The advantage of the antenna design presented here over the others summarized in Table 3 is that it has a wider bandwidth with higher gain range within the frequency range of interest for PD events, especially when small radiative sources (as holes and seams) are concerned. In addition, the innovative antenna design has a compact size that can enable it to fit in dielectric windows of some power apparatus, such as transformers and GIS for continuous PD monitoring.

IV. EXPERIMENTAL VALIDATION AND RESULTS

A. SURFACE DISCHARGE DETECTION IN AIR INSULATION USING THE DESIGNED ANTENNA AND THE COMMERCIAL HFCT SENSOR

To evaluate the antenna sensitivity performance, the fabricated UHF antenna was applied to detect surface PD activity on the epoxy resin PCB insulator made of FR-4 epoxy resin substrate whose permittivity value lies in the range of 4.3-5.0. The test specimen has dimension 100mm × 100mm × 1.6mm. The FR-4 epoxy resin substrate is partially covered by a copper foil (80 mm diameter, 0.035mm thick) which generates a non- homogenous electric field that, under high voltage stress, induces partial discharges on the resin surface. HV and ground test electrodes are cylindrical steel plates with diameter 65 mm and thickness 5 mm; see Fig. 9 and Fig.10 depicting the experimental PD measurement se-up for surface discharge. A typical PD measurement setup used in the laboratory experiment consists of the following components: a power supply (220VAC), a voltage regulator (in the range of 0-220V), a 100kV-5kVA high Voltage test transformer (step up transformer), a limiting resistor (6100-Ohm), a coupling capacitor (100pF), a voltage divider capacitor (40nF), a test

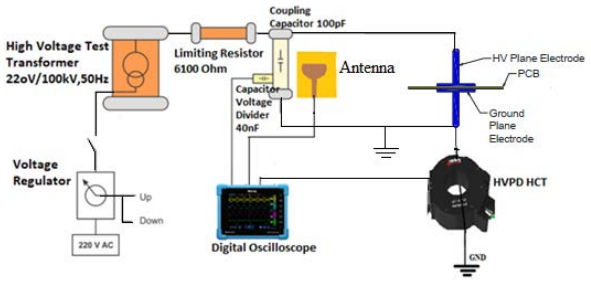

FIGURE 9. Schematic layout for PD measurement circuit components used to generate partial discharges on the epoxy resin PCB surface.

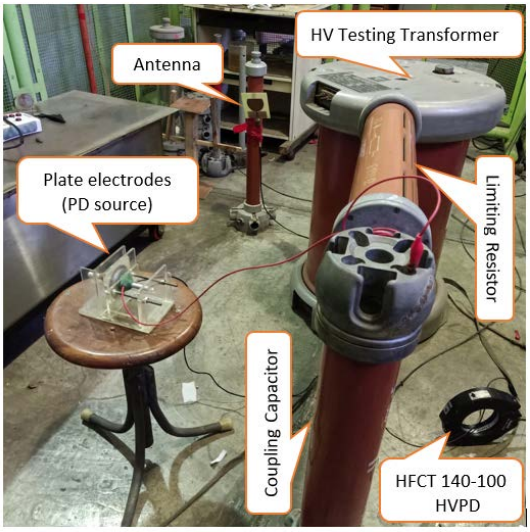

FIGURE 10. Experimental set-up for surface discharge measurement using the optimized innovative UHF antenna and the commercial HFCT sensor.

sample (insulation defect model), the designed UHF antenna, the commercial HFCT sensor and a digital storage oscilloscope (DSO). 50-Ohm lossless coaxial cables (5 meters long each) were used to connect the designed antenna and the HFCT to the digital oscilloscope where the detected PD signals were displayed and recorded by the oscilloscope.

To investigate the sensor's detection sensitivity, the antenna was placed at various positions from the PD source (plate electrodes), i.e. at 50, 70 and 100cm. The commercial HFCT sensor, clamped across the ground wire, was used as a target PD sensor to validate the designed antenna capability. Three test voltages, namely 5kV, 6kV and 7kV, were applied, and PD measurements were performed at room a temperature (25°C-27°C).

Partial discharge inception voltage (PDIV), phase-resolved PD (PRPD) pattern, PD magnitude and PD number (PD repetition rate in both positive and negative half-cycle) were recorded at each applied voltage and distance [32].

1) BACKGROUND NOISE MEASUREMENT

The background noise (BGN) was measured before conducting PD measurement experiments, see Table 4 that reports the average background noise level measured by using the

TABLE 4. Background noise (BGN) amplitudes detected by the UHF antenna and HFCT sensor under voltage (ON) and with no voltage (OFF).

Sensor	Average BGN OFF			Average BGN ON		
	Vmax (mV)	Vmin (mV)	Vpp (mV)	Vmax (mV)	Vmin (mV)	Vpp (mV)
HFCT	4.8	-3.2	8	4.8	-3.2	8
Antenna	4.8	-3.4	8.2	4.8	-4	8.8

designed antenna and the HFCT sensor. The average value was calculated from 30 data samples. The minimum, maximum and peak-to-peak voltage (Vpp) of the detected noise signal are given. It is clearly observed that the Vpp for the background noise measured by the HFCT and the antenna are 8mV and 8.2mV, respectively when the power supply was still in OFF mode (BGN OFF), being about the same, i.e. 8mV and 8.8mV, for both sensors, respectively when the power supply is switched ON (BGN ON). The trigger level on the oscilloscope was set near to the background noise level (±8.8mV) to prevent the signal acquisition from being triggered by the noise, but instead by partial discharge pulse signals. In case of non-repetitive, transient noise that exceeds the trigger level, it is removed by wavelet transform tools [33].

2) PARTIAL DISCHARGE INCEPTION VOLATAGE (PDIV) MEASUREMENT

To measure the partial discharge inception voltage (PDIV), the applied voltage was gradually increased until the PD pulse signals (whose amplitude is higher than that of the background noise) repeatedly appeared on the oscilloscope. Table 5 shows the average PDIV values alongside the PD pulse signal amplitudes (Vpp) for surface discharges detected by the designed UHF antenna placed at a distance of 50cm, 70cm, and 100cm from the plate electrodes (PD source), respectively. From these PDIV results, it is seen that the antenna positioned at 50cm from the PD source captures PD pulse signals with higher sensitivity, as expected, than when it is positioned at 70cm and 100cm from the PD source because, at an inception voltage of 2.5kV, the antenna positioned at 50cm detected a PD pulse amplitude of 424mV. However, the proposed optimized antenna has still a high sensitivity when placed at a distance of 100cm from the PD source, as PDIV and PD pulse magnitude have very slight increase and decrease, respectively. On the other hand, the HFCT sensor detects PD pulses at an inception voltage of 3.5kV with pulse amplitude of 1130mV, being thus, inferior, as regards sensitivity, to the designed antenna. It can also be mentioned that by increasing the distance between the antenna and the PD source, the partial discharge inception voltage (PDIV) increases at some extents while the PD pulse amplitudes detected at PDIV decreases when the antenna is positioned farther from the PD source.

3) BREAKDOWN VOLTAGE MEASUREMENT

The breakdown voltage (BDV) of the air under a uniform electric field using the test assembly of Fig. 9 was measured

TABLE 5. Average PDIV and PD pulse amplitudes for HFCT and the designed UHF antenna at different positions from PD source.

Sensor	Average PDIV (kV)	Average (Vpp) amplitude of the detected PD pulse signal	Positive Peak voltage (Vmax)	Negative peak voltage (Vmin)
Antenna at 50cm	2.5kV	420mV	156mV	-268mV
Antenna at 70cm	2.6kV	410mV	160mV	-250mV
Antenna at 100cm	2.7kV	370mV	96mV	-280mV
HFCT	3.5kV	1130mV	550mV	-580mV

TABLE 6. Comparison of mean values of PD pulse amplitudes detected by the HFCT sensor and the antenna at 5kV, k6V and 7kV with different antenna positions from the PD source.

Antenna position from the PD source	Antenna		
	Applied voltage		
	5kV	6kV	7kV
	Peak-to-peak voltage of detected PD pulse (mV)	Peak-to-peak voltage of detected PD pulse (mV)	Peak-to-peak voltage of detected PD pulse (mV)
50cm	584	624	696
70cm	512	600	672
100cm	496	576	664
HFCT Sensor			
HFCT positioned at fixed position across the ground wire	Applied voltage		
	5kV	6kV	7kV
	Peak-to-peak voltage of detected PD pulse signal (V)	Peak-to-peak voltage of detected PD pulse (V)	Peak-to-peak voltage of detected PD pulse (V)
	1.31	1.48	1.6

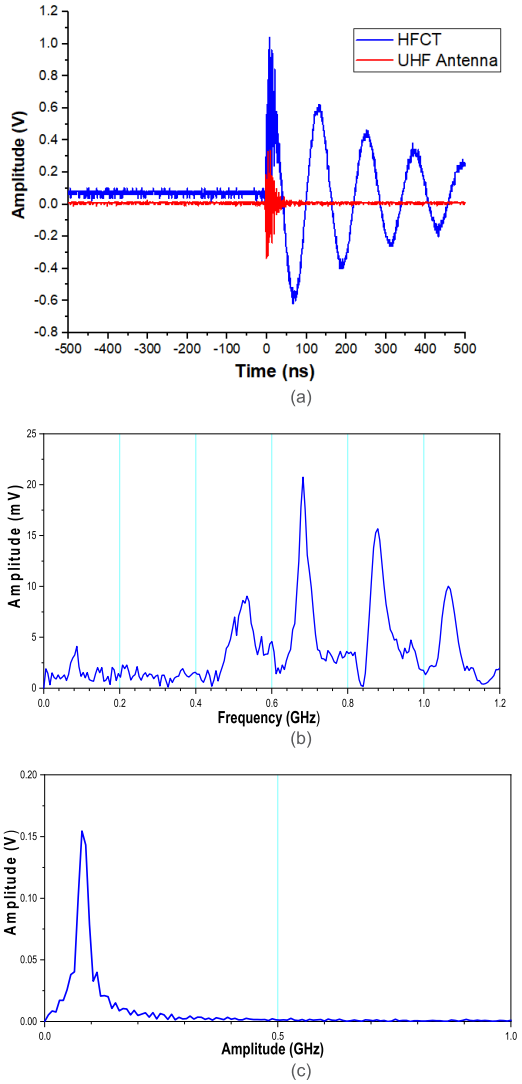

FIGURE 11. Typical (a) time-domain PD signal waveforms for surface discharge in air detected by the antenna placed at 100cm from the PD source simultaneously with the HFCT sensor at 7kV AC applied voltage (b) and (c) frequency spectrum of surface discharge in air detected by the antenna and the HFCT respectively.

before establishing the voltage test levels for PD measurements. The breakdown voltage due to the surface flashover at the interface between FR-4 epoxy resin insulator and air was 8.5kV (mean of 5 values). Therefore, the test applied voltages were chosen to be 5, 6, 7 kV, being between PDIV and BDV. Note that the breakdown voltage was measured under ambient pressure, ambient relative humidity and ambient temperature.

4) PARTIAL DISCHARGE WAVEFORM AMPLITUDE MEASUREMENT

The test voltage was increased gradually above the PDIV measuring the peak-to-peak voltage (Vpp) of PD waveforms.

Fig.11 (a) displays typical PD signal waveforms captured simultaneously by the commercial HFCT and the designed UHF antenna placed at a distance of 100cm from the PD source when the test voltage applied to the plate electrodes was 7kV. From Fig 11 (a), it is seen that the peak-to-peak voltage (Vpp) for the PD signal detected by the HFCT sensor is 1.6V while the Vpp detected by the designed UHF antenna is 664mV.

Table 6 summarizes the PD measurement results acquired by using the fabricated antenna prototype and the HFCT (commercial HVPD sensor), varying voltage and distance. It is confirmed that the optimized UHF antenna is capable of detecting the PD pulse signals radiated by the defective insulation under high electric field stress (PD activity) in HV and MV power equipment, with comparable sensitivity with respect to the HFCT sensor. It is noteworthy that, due to the antenna high gain and directivity in the ultra-wide band frequency (as seen in Fig.5), it can still have a high sensitivity, with a high signal-to-noise ratio, even when it is placed at distances $\geq$ 100cm from the PD source.

UHF antenna and HFCT are both sensitive to PD signals, but in different ways. Any comparison between these sensors (UHF antenna and HFCT) is purely qualitative, having the

purpose to assess the feasibility of PD detection through electromagnetic method (by detecting the irradiated PD signals, antenna) and near field coupling method (by detecting the PD pulse current flowing to the ground conductor, HFCT). Indeed, Fig. 11 (a) shows that the waveform and amplitude of the time-domain PD pulse signals captured by the designed UHF antenna and the commercial HFCT sensor differ because their modes of detection are also different.

The reason is that a HFCT sensor clamped across the ground wire detects the impulse current circulating in the PD measurement circuit and flowing to the ground (conducted current), thus dumping significantly (with distance) the highest- frequency components of a PD pulse. On the contrary, antenna senses irradiated PD-induced electromagnetic signals, which also attenuate with distance, but tend to keep the spectrum components.

For further analysis of PD characteristics detected by the proposed UHF antenna, the frequency spectrum of the PD signals captured by the UHF antenna and HFCT sensor are shown for both surface discharge in air insulation and corona discharge in oil insulation. The Fast Fourier Transformer (FFT) was used to obtain the associated frequency spectrum of the detected time-domain PD signals. Figure 11 (a) depicts the time-domain PD pulse signals, while Fig.11 (b) and (c) show, respectively, the corresponding frequency spectra of the PD signals detected by the UHF antenna and the HFCT in air insulation. It comes out that the frequency components of surface discharge signals in air insulation detected using the UHF antenna ranges from 100MHz to 1.2GHz, where the dominant frequency is mainly concentrated around 0.6GHz, Fig.11 (b). On the other hand, the frequency spectrum of the PD signal detected by the HFCT sensor in air insulation ranges from 0 to 120MHz, with dominant frequency observed around 100MHz, as seen in Fig.11(c).

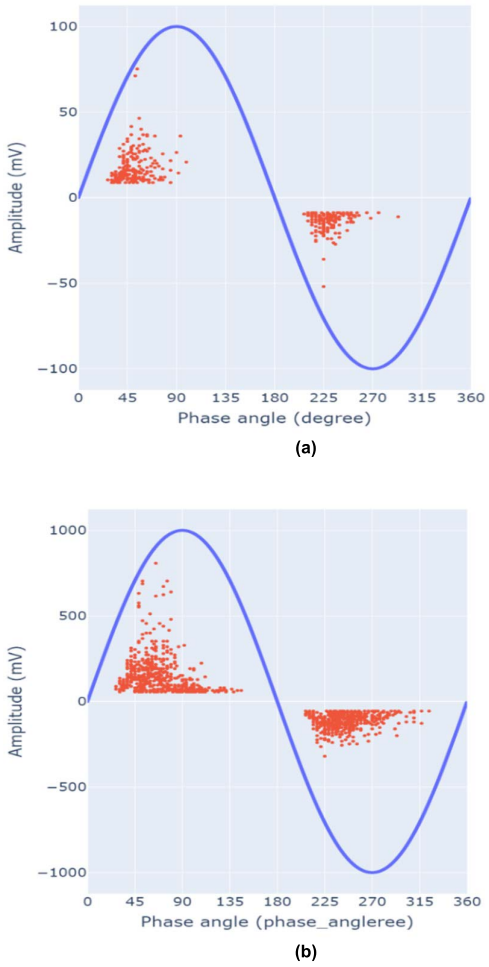

FIGURE 12. PRPD patterns of surface discharge detected at 5kV using (a) Antenna (b) HFCT.

5) PHASE RESOLVED PARTIAL DISCHARGE PATTERN

The Phase resolved partial discharge (PRPD) pattern is a fundamental tool used to understand and analyze the type of partial discharge source generating PD (thus their severity in causing accelerated aging). The PRPD pattern summarizes the PD phenomenology in terms of phase – amplitude – number (ϕ – V – N) characteristics. Each point within a PRPD pattern represents individual PD events caused by the discharging defect within the insulation system.

In the experiments reported here, PRPD patterns are typical of surface discharges, according to test arrangement purposes. The collection of PRPD patterns was carried out through 100 cycles of the applied 50Hz sinusoidal voltage. From PRPD patterns presented in Fig.12-Fig.14, it is seen that they carry the same analysis and diagnostic message for both antenna and HFCT, being structured in a way that an expert would easily associate the patterns to that of surface discharges [34], [35], [36].

More references about the PRPD for surface discharge including surface discharge on Epoxy Resin, the solid insulation used in this paper, can be found in literature, e.g. [37], [38], [39], [40], [41], [42], [43], [44], [45], and [46].

Indeed, by increasing the applied voltage, the discharge number and discharge amplitude in both positive and negative half-cycles will increase accordingly for both antenna and HFCT sensor. It can also be seen that the PD pulses number in both positive and negative half cycles are almost equal in number and symmetrical for the designed antenna and HFCT sensor. On the whole, it can be speculated that the designed UHF antenna is capable of recognizing the type of insulation defects generating PD in the same manner as the commercial HFCT sensor.

B. CORONA DISCHARGE DETECTION IN OIL INSULATION

To further investigate the sensitivity performance of the optimized antenna for PD detection in oil-insulated systems, PD measurements in oil insulation were performed by using simultaneously the antenna and commercial HFCT. Fig.15 depicts the experimental set-up used for PD detection in transformer mineral oil. A plastic container filled with transformer

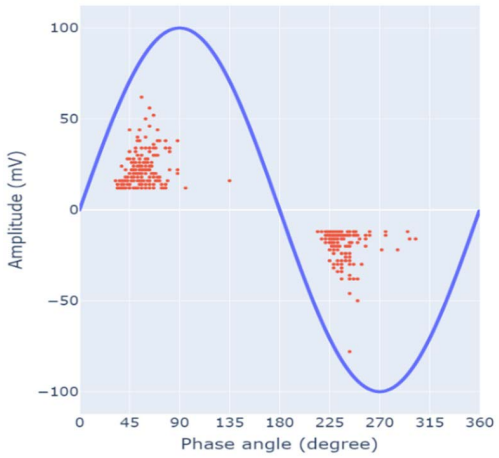

(a)

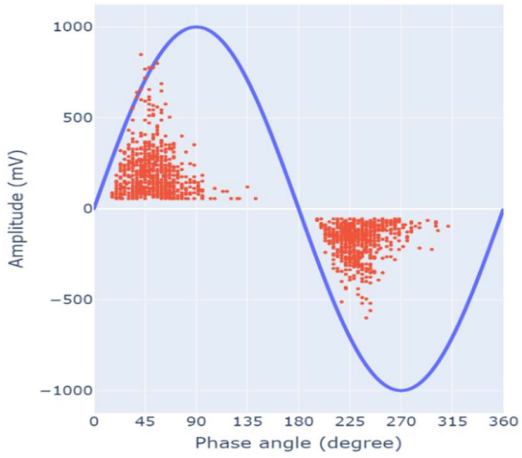

(b)

FIGURE 13. PRPD patterns of surface discharge detected at 6kV using (a) Antenna (b) HFCT.

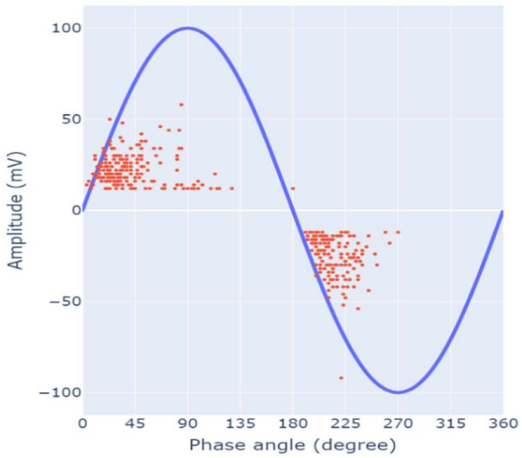

(a)

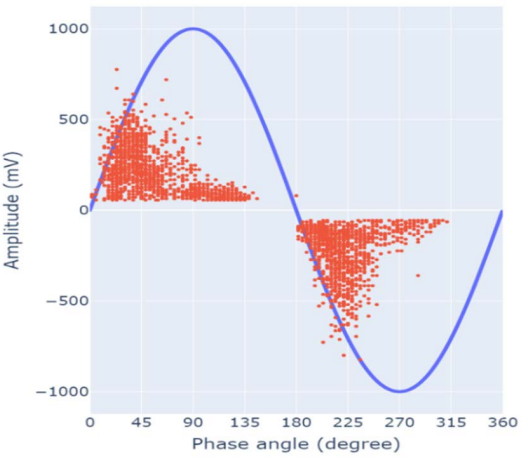

(b)

FIGURE 14. PRPD patterns of surface discharge detected at 7kV using (a) Antenna (b) HFCT.

oil was used, in which a needle-plate electrode system was placed to generate corona discharge in oil. The needle electrode was connected to the HV lead of the transformer while the plate electrode was connected to the ground wire. The gap distance between the needle edge and the circular plate electrode was fixed to 10mm. During this experiment, the position of the designed UHF antenna was 100cm away from the PD source (test object).

Before starting PD measurements, the background noise level in the laboratory was measured showing again an average peak-to-peak voltage of 8mV and 8.8mV for HFCT and antenna, respectively.

Partial discharge inception voltage (PDIV) and breakdown voltage (BDV) were also measured to help setting the test voltages. The PDIV measured using the designed antenna was 7.2kV, very close to that obtained by the HFCT, i.e. 7.6kV. The breakdown voltage in oil was measured to be 20kV. It is worth mentioning that the PDIV and breakdown

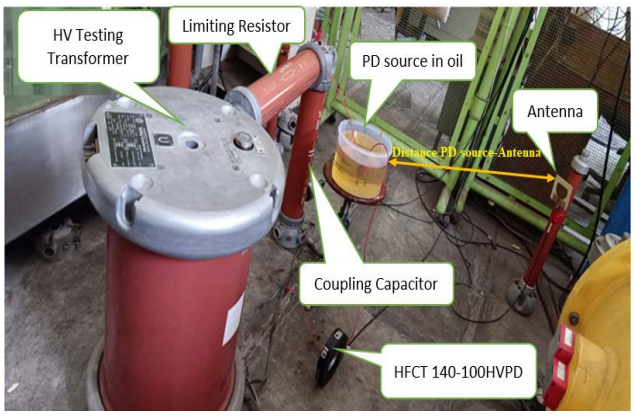

FIGURE 15. Experimental set-up for PD detection in transformer oil using the designed UHF antenna and the commercial HFCT sensor.

voltage using the needle-plate electrode model in oil highly depends on the gap distance between the needle tip and the

TABLE 7. Comparison of PD pulse magnitudes detected by the commercial HFCT sensor and designed UHF antenna in transformer oil insulation at 10kV, 12kV and 14kV when the antenna was positioned at a distance of 100cm from the PD source.

Applied voltage	PD pulse signal magnitude (Vpp) detected by the designed UHF antenna	PD pulse signal magnitude (Vpp) detected by the commercial HFCT sensor
10kV	38.4mV	35.2mV
12kV	69.6mV	66.4mV
14kV	81.6mV	62.4mV

plate electrode: the shorter is the gap distance, the lower are the PDIV and the breakdown voltages.

Three test voltages, namely 10kV, 12kV and 14kV, were thus applied to the test cell to collect PD data detected by the designed antenna and the HFCT sensor. Values of PD magnitude for different voltage levels and different sensors are summarized in Table 7.

Based on PD signals magnitude presented in Fig.16 and Table 7, It is evident that the optimal designed of the proposed UHF antenna has a higher sensitivity, compared to that of the HFCT sensor. Once more, the PD waveform detected by the antenna is different from that detected by the HFCT, see Fig. 16 (a), but this does not affect the overall antenna sensitivity and performance. Indeed, then optimized antenna has high signal-to-noise ratio (SNR) enabling the antenna to suppress the ambient electromagnetic interferences when used in a noisy environment, such as in the substation. As it is seen from Fig.16 (a), the designed antenna has detected a PD pulse signal whose amplitude is 81.6mV as indicated in red color waveform trace. Since we know the value of background noise level detected by the same antenna was 8.8mV, therefore we can estimate the signal-to-noise ratio (SNR) of the designed antenna to be equal to (81.6mV/ 8.8mV$=$ 9.3), this estimation was also used in the literature [19]. This clearly justifies that the designed antenna has a high SNR and signal integrity to detect PD signals with high sensitivity when it is even positioned at a distance $\geq$ 100cm from the PD source.

Additionally, the frequency spectrum of corona discharge in oil insulation was analyzed. Figure 16 (a) shows the time-domain PD waveform while Fig.16 (b) and (c) depict, respectively, the corresponding frequency spectrum of the PD signals detected by antenna and HFCT in transformer oil. It is clearly observed that the frequency content for corona discharge signals in oil insulation detected using the UHF antenna ranges from 400MHz to 1.2GHz, where the dominant frequency is mainly concentrated around 0.5GHz, Fig.16 (b). On the contrary, the frequency spectrum for PD signal detected by the HFCT sensor in oil insulation goes from 0 to 100MHz, with the dominant frequency around 80MHz, as seen in Fig.16(c). It is worth mentioning that the frequency spectrum of the detected PD signals strongly depends on the type of insulation defect (PD source), propagation medium and the operating frequency band of the UHF antenna or HFCT used.

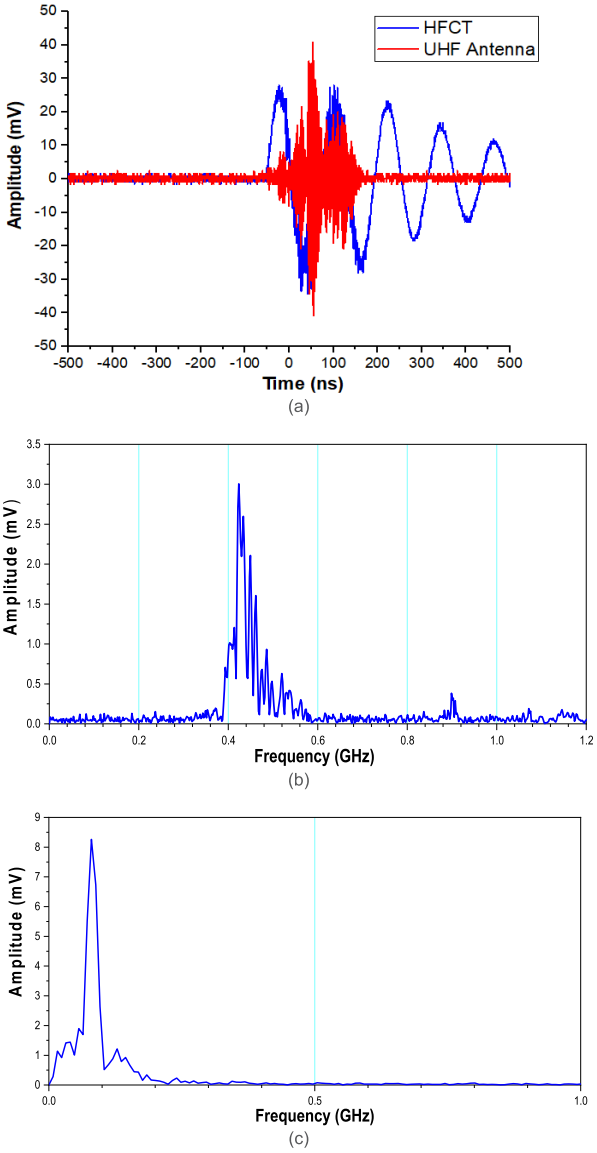

FIGURE 16. Typical (a) time-domain PD signal waveforms for corona discharge in oil detected by the antenna placed at 100cm from the PD source simultaneously with the HFCT sensor at 14kV AC applied voltage (b) and (c) frequency spectrum of corona discharge in oil detected by the antenna and the HFCT respectively.

V. CONCLUSION

A UHF antenna, derived from a circular microstrip patch antenna, has been proposed for partial discharge detection on high voltage (HV) and medium voltage (MV) power assets. The proposed UHF antenna has a frequency band of 1.2GHz-4.5GHz, covering a total bandwidth of 3.3GHz with a return loss less than $-$10dB in the entire antenna's operating frequency. It has a compact size of 100mm $\times$ 100 mm $\times$ 1.6mm.

The simulation and measurement results of this antenna are in a good agreement. The proposed antenna has a VSWR value $<$ 2 (close to 1 within the operating frequency band), confirming its good impedance matching when connected to a transmission line (e.g. 50Ω-coaxial cable linking the antenna to the oscilloscope).

To validate the detection sensitivity performance, the designed antenna was used for PD detection and measurement through laboratory experiments by using two types of test objects. One experiment was conducted in air, with an object consisting of a FR-4 epoxy insulation slab inserted between two parallel plates electrodes able to generate partial discharges on the insulator surface. Another experiment was performed in mineral oil insulation using a needle-plate electrode arrangement to generate corona discharges in oil. In all experiments, the designed antenna was used simultaneously with the commercial HFCT sensor, used as a comparison PD sensor. Various supply voltage values and antenna distances from the PD source were considered for sensitivity performance purposes.

On the whole, the antenna proved to have a high sensitivity even when placed at a distance of 100cm from the PD source. Moreover, the antenna shows high sensitivity and high signal-to-noise ratio (SNR), due to its high gain and high directivity allowing a good suppression of the external interferences (noise) present in the surrounding environment. In addition, based on the PRPD patterns acquisition for the designed antenna and the commercial HFCT sensor, it was observed that the designed antenna has been able to recognize the insulation defect (surface discharge in air) in the same way as the HFCT sensor. Moreover, based on the frequency spectrum of the surface discharge signal in air insulation and corona discharge in oil detected by the designed antenna, it is evident that the detected PD signals lies in the UHF range.

In conclusion, the optimized design of UHF antenna presented in this article shows the potential to be a valid candidate UHF PD sensor that can be employed for the diagnosis of the air-insulated and oil-insulated HV and MV power assets.

REFERENCES

[1] R. Ghosh, P. Seri, R. E. Hebner, and G. C. Montanari, "Noise rejection and detection of partial discharges under repetitive impulse supply voltage," *IEEE Trans. Ind. Electron.*, vol. 67, no. 5, pp. 4144–4151, May 2020.

[2] X. Chen, Y. Qian, Y. Xu, G. Sheng, and X. Jiang, "Energy estimation of partial discharge pulse signals based on noise parameters," *IEEE Access*, vol. 4, pp. 10270–10279, 2017.

[3] S. Suwarno, "Partial discharge in high voltage insulating materials," *Int. J. Electr. Eng. Informat.*, vol. 8, no. 1, pp. 147–163, Mar. 2016.

[4] G. C. Montanari, P. Seri, P. Morshuis, and R. Hebner, "An approach to insulation condition monitoring and life assessment in emerging electrical environments," *IEEE Trans. Power Del.*, vol. 34, no. 4, pp. 1357–1364, Aug. 2019.

[5] U. Khayam, W. A. Putro, K. Urano, C. Min, M. Kozako, and M. Hikita, "Partial discharge pattern of various defects measured by spiral antenna as UHF external sensor on 66 kV GIS model," *Int. J. Electr. Eng. Informat.*, vol. 6, no. 2, pp. 404–420, Jun. 2014.

[6] S. Lu, H. Chai, A. Sahoo, and B. T. Phung, "Condition monitoring based on partial discharge diagnostics using machine learning methods: A comprehensive state-of-the-art review," *IEEE Trans. Dielectr. Electr. Insul.*, vol. 27, no. 6, pp. 1861–1888, Dec. 2020.

[7] S. Park and K. Y. Jung, "Design of a circularly-polarized UHF antenna for partial discharge detection," *IEEE Access*, vol. 8, pp. 81644–81650, 2020.

[8] S. Anjum, S. Jayaram, A. El-Hag, and A. N. Jahromi, "Detection and classification of defects in ceramic insulators using RF antenna," *IEEE Trans. Dielectr. Electr. Insul.*, vol. 24, no. 1, pp. 183–190, Feb. 2017.

[9] S.-G. Ha, J. Cho, J. Lee, B.-W. Min, J. Choi, and K.-Y. Jung, "Numerical study of estimating the arrival time of UHF signals for partial discharge localization in a power transformer," *J. Electromagn. Eng. Sci.*, vol. 18, no. 2, pp. 94–100, Apr. 2018.

[10] H. Chai, B. T. Phung, and S. Mitchell, "Application of UHF sensors in power system equipment for partial discharge detection: A review," *Sensors*, vol. 19, no. 5, p. 1029, 2019.

[11] J. M. Neto, Y. Zhang, A. Jaber, M. Zhu, M. Judd, R. Atkinson, J. Soraghan, J. S. Neto, Q. V. M. de Fatima, and I. A. Glover, "Radiometric location of partial discharge sources for the future smart grid," in *Proc. 31st URSI Gen. Assem. Sci. Symp. (URSI GASS)*, Aug. 2014, pp. 1–4.

[12] X. Zhang, Z. Cheng, and Y. Gui, "Design of a new built-in UHF multi-frequency antenna sensor for partial discharge detection in high-voltage switchgears," *Sensors*, vol. 16, no. 8, p. 1170, 2016.

[13] H. F. Ye, Q. Yong, D. Yue, G. H. Sheng, and X. C. Jiang, "Development of multi-band ultra-high-frequency sensor for partial discharge monitoring based on the meandering technique," *IET Sci. Meas. Technol.*, vol. 8, no. 5, pp. 327–335, 2014.

[14] D. S. Kim, C.-M. Hwang, Y.-N. Kim, J.-O. Choi, W.-B. Seo, B.-S. Han, S.-H. Choi, and Y.-M. Jang, "Development of an intelligent spacer built into the internal-type UHF partial discharge sensor," in *Proc. Conf. Rec. IEEE Int. Symp. Electr. Insul.*, vol. 1, Jun. 2008, pp. 396–399.

[15] M. D. Judd, "Experience with UHF partial discharge detection and location in power transformers," in *Proc. Elect. Insul. Conf. (EIC)*, Jun. 2011, pp. 201–205.

[16] Y. Qi, Y. Fan, G. Bing, R. Jia, W. Sen, S. Wei, and A. Jadoon, "Design of ultra-wide band metal-mountable antenna for UHF partial discharge detection," *IEEE Access*, vol. 7, pp. 60163–60170, 2019.

[17] T. Li, M. Rong, C. Zheng, and X. Wang, "Development simulation and experiment study on UHF partial discharge sensor in GIS," *IEEE Trans. Dielectr. Electr. Insul.*, vol. 19, no. 4, pp. 1421–1430, Aug. 2012.

[18] A. A. Zahed, A. H. El-Hag, N. Qaddoumi, R. Hussein, and K. B. Shaban, "Comparison of different fourth order Hilbert fractal antennas for partial discharge measurement," *IEEE Trans. Dielectr. Electr. Insul.*, vol. 24, no. 1, pp. 175–182, Feb. 2017.

[19] P. Wang, S. Ma, S. Akram, K. Zhou, Y. Chen, and M. T. Nazir, "Design of archimedes spiral antenna to optimize for partial discharge detection of inverter fed motor insulation," *IEEE Access*, vol. 8, pp. 193202–193213, 2020.

[20] J.-S. Kuo and G.-B. Hsieh, "Gain enhancement of a circularly polarized equilateral-triangular microstrip antenna with a slotted ground plane," *IEEE Trans. Antennas Propag.*, vol. 51, no. 7, pp. 1652–1656, Jul. 2003.

[21] P. P. Chandran and S. Viswasom, "Gain and bandwidth optimization of a novel microstrip patch antenna," in *Proc. 4th Int. Conf. Adv. Comput. Commun. (ICACC)*, 2014, pp. 315–318.

[22] D. S. Marotkar and P. Zade, "Bandwidth enhancement of microstrip patch antenna using defected ground structure," in *Proc. Int. Conf. Elect., Electron., Optim. Techn. (ICEEOT)*, Mar. 2016, pp. 1712–1716.

[23] S. Kumari, S. Sachan, and A. Rajawat, "Bandwidth enhancement of microstrip patch antenna using disconnected U-shaped DGS," in *Intelligent Communication, Control and Devices* (Advances in Intelligent Systems and Computing), vol. 624, R. Singh, S. Choudhury, and A. Gehlot, Eds. Singapore: Springer, 2018, doi: 10.1007/978-981-10-5903-2_106.

[24] J. P. Uwiringiyimana, U. Khayam, and G. C. Montanari, "Design and implementation of ultra-wide band antenna for partial discharge detection in high voltage power equipment," *IEEE Access*, vol. 10, pp. 10983–10994, 2022.

[25] H. Chai, B. T. Phung, and D. Zhang, "Development of UHF sensors for partial discharge detection in power transformer," in *Proc. Condition Monitor. Diagnosis (CMD)*, Sep. 2018, pp. 1–5.

[26] A. Munir, G. Petrus, and H. Nusantara, "Multiple slots technique for bandwidth enhancement of microstrip rectangular patch antenna," in *Proc. Int. Conf. QiR*, Jun. 2013, pp. 150–154.

[27] Y. Rahayu, T. A. Rahman, R. Ngah, and P. S. Hall, "Slotted ultra wideband antenna for bandwidth enhancement," in *Proc. Loughborough Antennas Propag. Conf.*, Mar. 2008, pp. 449–452.

[28] J. Li, P. Wang, T. Jiang, L. Bao, and Z. He, "UHF stacked Hilbert antenna array for partial discharge detection," *IEEE Trans. Antennas Propag.*, vol. 61, no. 11, pp. 5798–5801, Nov. 2013.

[29] Z. Cui, S. Park, H. Choo, and K.-Y. Jung, "Wideband UHF antenna for partial discharge detection," *Appl. Sci.*, vol. 10, no. 5, p. 1698, Mar. 2020.

[30] P. Wang, S. Ma, S. Akram, P. Meng, J. Castellon, Z. Li, and G. C. Montanari, "Design of an effective antenna for partial discharge detection in insulation systems of inverter-fed motors," *IEEE Trans. Ind. Electron.*, vol. 69, no. 12, pp. 13727–13735, Dec. 2021.

[31] F. Bin, F. Wang, Q. Sun, S. Lin, Y. Xie, and M. Fan, "Internal UHF antenna for partial discharge detection in GIS," *IET Microw., Antennas, Propag.*, vol. 12, no. 14, pp. 2184–2190, Nov. 2018.

[32] C. Ma, H. Li, W. Zhou, J. Yu, L. Wang, S. Yang, and S. Hu, "Background noise of partial discharge detection and its suppression in complex electromagnetic environment," in *Proc. IEEE Int. Conf. High Voltage Eng. Appl. (ICHVE)*, Sep. 2018, pp. 1–4.
[33] J. P. Uwiringiyimana and U. Khayam, "Noise measurement in high voltage laboratory by using high frequency current transformer and loop antenna," in *Proc. Int. Conf. High Voltage Eng. Power Syst. (ICHVEPS)*, Oct. 2017, pp. 35–39.
[34] A. R. Mor, L. C. C. Heredia, D. A. Harmsen, and F. A. Muñoz, "A new design of a test platform for testing multiple partial discharge sources," *Int. J. Elect. Power Energy Syst.*, vol. 94, pp. 374–384, Jan. 2018.
[35] A. Rodrigo-Mor, F. Muñoz, and L. Castro-Heredia, "A novel antenna for partial discharge measurements in GIS based on magnetic field detection," *Sensors*, vol. 19, no. 4, p. 858, Feb. 2019.
[36] T. Luo, W. Zhao, and M. G. Niasar, "Experimental study of epoxy surface discharge under different frequencies," in *Proc. IEEE Conf. Electr. Insul. Dielectr. Phenomena (CEIDP)*, Dec. 2021, pp. 574–577.
[37] R. P. Nair and B. V. Sumangala, "Classification of partial discharge sources in mica-epoxy-glass insulation sample using statistical analysis," *Power Res.*, vol. 13, no. 1, pp. 19–24, 2018.
[38] J. Zhang, T. Yao, T. Shahsavarian, C. Li, Z. Lei, Z. Zhang, R. Jia, and S. Diaham, "Improvement in anti-static property and thermal conductivity of epoxy resin by doping graphene," *IEEE Trans. Dielectr. Electr. Insul.*, vol. 27, no. 2, pp. 542–548, Apr. 2020.
[39] D. Verginadis, A. Karlis, M. G. Danikas, and J. A. Antonino-Daviu, "Investigation of factors affecting partial discharges on epoxy resin: Simulation, experiments, and reference on electrical machines," *Energies*, vol. 14, no. 20, p. 6621, Oct. 2021, doi: 10.3390/en14206621.
[40] R. Sarathi, S. Aravinth, and K. Sethupathi, "Analysis of surface discharge activity in epoxy nanocomposites in liquid nitrogen under AC voltage," *IEEE Trans. Dielectr. Electr. Insul.*, vol. 21, no. 2, pp. 452–459, Apr. 2014.
[41] A. Kang, M. Tian, C. Li, J. Song, S. V. Suraci, W. Li, L. Lin, Z. Lei, and D. Fabiani, "Development and pattern identification of end-winding discharge under effect of relative humidity and temperature for HV motors," *High Voltage*, vol. 5, no. 4, pp. 434–443, Aug. 2020.
[42] B. I. Ayubi, L. Zhang, H. Xu, and Q. Yan, "Surface discharge characteristics and influencing factors of polyimide insulations under high-frequency sinusoidal voltages," *IET Gener., Transmiss. Distrib.*, vol. 16, no. 5, pp. 1000–1012, Mar. 2022.
[43] J. A. A. Rey, R. A. Sánchez, and G. Robles, "A new monitoring and characterization system of partial discharges based on the analysis of the spectral power," *Ingeniería Investigación*, vol. 35, no. 1, pp. 13–20, Nov. 2015.
[44] A. Pfeffer, S. Tenbohlen, and S. Kornhuber, "Pulse-sequence analysis of partial discharges in power transformers," in *Proc. 17th Int. Symp. High Voltage Eng.*, Dec. 2011, pp. 1–5.
[45] S. A. Madhar, A. R. Mor, P. Mraz, and R. Ross, "Study of DC partial discharge on dielectric surfaces: Mechanism, patterns and similarities to AC," *Int. J. Electr. Power Energy Syst.*, vol. 126, Mar. 2021, Art. no. 106600.
[46] Y. Xia, X. Song, J. He, Z. Jia, and X. Wang, "Simulation and partial discharge detection for typical defects of 10 kV cable the joint," *J. Eng.*, vol. 2019, no. 16, pp. 2856–2859, Mar. 2019.

JEAN PIERRE UWIRINGIYIMANA received the B.Sc. degree in electrical engineering from the National University of Rwanda, Rwanda, in 2013, and the M.Sc. degree in electrical engineering from the Institut Teknologi Bandung, Bandung, Indonesia, in 2019, where he is currently pursuing the Ph.D. degree in electrical engineering. He has published several conference papers and journal articles in the field of high voltage engineering. His current research interests include partial discharge diagnosis on high voltage power apparatuses, development of UHF sensors for partial discharge monitoring on high voltage power apparatuses, and condition monitoring of high voltage power equipment based on partial discharge measurement technique.

UMAR KHAYAM (Member, IEEE) received the B.Sc. and M.Sc. degrees from the Department of Electrical Engineering, Institut Teknologi Bandung, Indonesia, in 1998 and 2000, respectively, and the Ph.D. degree from the Kyushu Institute of Technology, Japan, in 2008. He is currently an Associate Professor with the Power Engineering Research Group, School of Electrical Engineering and Informatics, Bandung Institute of Technology (ITB), Indonesia. He is also the Head of the High Voltage and High Current Engineering Laboratory and the Head of Doctoral Study Program of Electrical Engineering and Informatics, ITB. He published more than 156 international conference papers and journal articles. His research interests include high voltage engineering, mainly on the development of diagnosis system of power apparatus based on partial discharge measurement technique. He received the best paper award from some international conferences, in 2005, 2014, 2016, and 2018.

SUWARNO (Senior Member, IEEE) received the B.Sc. and M.Sc. degrees from the Department of Electrical Engineering, Institut Teknologi Bandung, Indonesia, in 1988 and 1991, respectively, and the Ph.D. degree from Nagoya University, Japan, in 1996. He is currently a Professor and the Emeritus Dean of the School of Electrical Engineering and Informatics Institut Teknologi Bandung. He is currently serving as the Head of Electrical Power Engineering Research Group, School of Electrical Engineering and Informatics, ITB. He has published over 260 international journal and conference papers. His research interests include high voltage insulating materials, technology, and diagnostics of HV equipment. He received the Student Best Awards from IEEJ Japan, in 1994 and 1995; from IEEE Queensland, Australia, in 1994; and from ACED Seoul, South Korea, in 2002. He was elected as The First Winner of Outstanding Indonesian Lecturer by The Ministry of Education and Culture, in 2009. He was the General Chairperson of several IEEE sponsored international conferences such as ICPADM 2006, ICEEI 2007, CMD 2012, ICHVEPS 2017, ICHVEPS 2019, and ICHVEPS 2021. He has been listed in top 2% of the world's most influential scientists according to a study conducted by Stanford University 2021. He is the Editor-in-Chief for the *International Journal on Electrical Engineering and Informatics.*

GIAN CARLO MONTANARI (Life Fellow, IEEE) is currently a Research Faculty III with the Center for Advanced Power Systems (CAPS), Florida State University, USA, and also a Alma Mater Professor with the Bologna University, Italy, and an Adjunct Professor at the Institut Teknologi Bandung, Indonesia. He has been a Full Professor of electrical technology with the Department of Electrical, Electronic and Information Engineering, University of Bologna, teaching courses on electrical technology, reliability, and asset management. Since 1979, he has been working in the field of aging and endurance of insulating materials and systems, diagnostics of electrical systems, asset management, and innovative electrical materials (magnetics, electrets, super-conductors, nano-materials). He has also been engaged in the fields of power quality and energy market, power electronics, reliability and statistics of electrical systems, and smart grid. He was the Founder and the President of the spin-off Techimp, established in 1999. He is the author or coauthor of more than 800 scientific papers. He has been recognized with several awards, including the IEEE Ziu-Yeda, Thomas W. Dakin, Whitehead, Eric Forster, and IEC 1906 Awards.